HAL
open science

Interface domain wall and exchange bias phenomena in ferrimagnetic/ferrimagnetic bilayers

S. Mangin, F. Montaigne, A. Schuhl

To cite this version:

S. Mangin, F. Montaigne, A. Schuhl. Interface domain wall and exchange bias phenomena in ferrimagnetic/ferrimagnetic bilayers. Physical Review B: Condensed Matter and Materials Physics (1998-2015), 2003, 68 (14), 10.1103/PhysRevB.68.140404 . hal-02104715

HAL Id: hal-02104715

https://hal.univ-lorraine.fr/hal-02104715v1

Submitted on 19 Apr 2019

HAL is a multi-disciplinary open access archive for the deposit and dissemination of scientific research documents, whether they are published or not. The documents may come from teaching and research institutions in France or abroad, or from public or private research centers.

L'archive ouverte pluridisciplinaire **HAL**, est destinée au dépôt et à la diffusion de documents scientifiques de niveau recherche, publiés ou non, émanant des établissements d'enseignement et de recherche français ou étrangers, des laboratoires publics ou privés.

PHYSICAL REVIEW B **68**, 140404(R) (2003)

Interface domain wall and exchange bias phenomena in ferrimagnetic/ferrimagnetic bilayers

S. Mangin, F. Montaigne, and A. Schuhl
Laboratoire de Physique des Matériaux, Université Nancy 1, Boîte Postale 239, F-54506 Vandoeuvre lès Nancy, France
(Received 12 May 2003; published 3 October 2003)

In $Gd_{40}Fe_{60}/Tb_{12}Fe_{88}$ exchange-coupled bilayer system, both negative and positive exchange bias, depending on cooling field, are observed. A full enlightenment of the magnetic configurations adopted by the system is obtained through micromagnetic calculations in agreement with magnetization and susceptibility measurements. Magnetization shifts and exchange bias fields are then quantitatively correlated to the presence of a frozen interface domain wall. This model may be transposed to antiferromagnetically exchange coupled antiferromagnetic/ferromagnetic (Fe/FeF_2 or Fe/MnF_2) systems

DOI: 10.1103/PhysRevB.68.140404 PACS number(s): 75.60.Ch, 75.30.Et, 75.50.Gg, 75.70.Cn

Exchange bias (EB) has been widely studied in ferromagnetic (FM)/antiferromagnetic (AFM) bilayers.[1,2] This phenomenon which is often essential for magnetoelectronic devices[3] is mainly characterized, below a blocking temperature T_B, by a shift of the M-H loop towards a field known as the exchange bias field H_E. In some FM/AFM systems exhibiting antiferromagnetic exchange coupling such as Fe/FeF_2 or Fe/MnF_2, it has been shown that a cooling field H_{fc} could trigger H_E from positive to negative values at low temperature and induce a magnetization shift.[4–6] Also strong correlation between H_{fc}, H_E and magnetization shift of the hysteresis loop has been observed.[5] Additionally several authors[6,7] pointed a peak in the coercive field H_C for H_E close to zero. Despite numerous studies, the mechanism leading to the EB effect is not yet fully understood. However, an estimation of the H_E must rely on configurations of the interface magnetization. Two different kinds of model are proposed. A first approach to model EB phenomena is based on the formation of lateral domains in the antiferromagnet resulting in the formation of lateral domain wall.[8] On the other hand, various models proposed the presence of an interface domain wall (iDW) with a modulation vector perpendicular to the interface. The position of the iDW (in AFM or in the FM) and its shape (90° or 180°) are up to now widely discussed.[9–11] These aspects are still in debate after 15 years of intensive research, mainly because the magnetic configuration inside the AFM layer is not measurable using classical magnetometric methods (at least linear) due to its zero net magnetization. Other exchange-coupled systems such as "spring magnet" made of two layers (ferromagnetic or/and ferrimagnetic) have shown EB effect.[12–14] The presence of an interface DW was clearly evidence in that case. However, the interface exchange coupling was *ferromagnetic* and only negative EB was observed.

In this paper, we have studied EB phenomena in an *antiferromagnetically* coupled ferrimagnetic/ferrimagnetic bilayer, namely, $Gd_{40}Fe_{60}/Tb_{12}Fe_{88}$. We present here the evolution of the magnetic properties (H_E, H_C, and magnetization shifts) of this system at low temperature depending on H_{fc}. Using ferrimagnetic layers, we investigated the magnetic configurations of both layers, and then develop a quantitative model for H_E and M^N_{Shift} variation of antiferromagnetically coupled bilayers. The $Gd_{40}Fe_{60}$(100 nm)/$Tb_{12}Fe_{88}$(50 nm) sample has been prepared by coevaporation on a glass substrate kept at 77 K and protected by a 30-nm Si capping layer.[12] Both $Gd_{40}Fe_{60}$ and $Tb_{12}Fe_{88}$ are ferrimagnetic alloys, Fe and rare-earth magnetic moments being very strongly antiferromagnetically coupled and thus antiparallel. In $Tb_{12}Fe_{88}$, the iron contribution to magnetization is dominant for all temperatures. This composition has been chosen to avoid the occurrence of a compensation temperature.[16] The terbium moments present a spreading of their direction because of the strong random local anisotropy. $Tb_{12}Fe_{88}$ becomes thus a hard magnetic alloy at low temperature because of the large increase of the terbium magnetic anisotropy. On the contrary, in $Gd_{40}Fe_{60}$, the contribution of gadolinium is dominant and the magnetization is locally parallel to that of the Gd moments (antiparallel to that of iron), the magnetic anisotropy is generated by the growth process and GdFe exhibits a very clear in-plane easy axis in the film plane.[17] This anisotropy remains weak at low temperatures because of the s character of the Gd $4f$ band. For all the measurements presented here, the magnetic field was applied in the sample plane along the GdFe easy axis. The exchange coupling between the layers being dominated by Fe-Fe ferromagnetic interactions, the magnetizations of GdFe and TbFe are antiferromagnetically coupled at the interface.

Equilibrium magnetic configurations have been calculated by using a simple unidimensional micromagnetic model.[13,14] Due to the demagnetizing field, the magnetization is kept in the plane of the layers and the magnetic profile is characterized by a single depth dependent angle $\theta(z)$ referred to the anisotropy direction. The magnetic energy of the bilayer per area unit is calculated by considering, for each layer (GdFe and TbFe): the exchange energy (characterized by the exchange stiffness A_{GdFe} or A_{TbFe}), the anisotropy energy (minimum for $\theta=0°$ and $\theta=180°$ and proportional to the anisotropy energy K_{GdFe} or K_{TbFe}), the Zeeman energy corresponding to the interaction of the magnetization M_{GdFe} or M_{TbFe} with the applied field H, and finally the interface exchange energy (characterized by a negative exchange stiffness J).

 ©2003 The American Physical Society

TABLE I. Magnetic parameters of a single layer (thickness t) $Gd_{40}Fe_{60}$ and $Tb_{12}Fe_{88}$ at 300 K and 5 K used to performed the micromagnetic simulations on the bilayer. (The interface coupling J has been taken to be -10^{-7} erg/cm^2). They are found to be in good agreement with the one obtained from measurements and calculations (Ref. 16).

Alloy	t (nm)	A (erg/cm)	K (erg/cm^3)	M (emu)
$Gd_{40}Fe_{60}$ (300 K)	100	6×10^{-7}	2.5×10^4	500
$Gd_{40}Fe_{60}$ (5 K)	100	6×10^{-7}	10^5	1000
$Tb_{12}Fe_{88}$ (300 K)	50	8×10^{-8}	2.8×10^4	225
$Tb_{12}Fe_{88}$ (5 K)	50	8×10^{-8}	$>10^7$	350

$$E=\int_0^{t_{\mathrm{GdFe}}}\left[A_{\mathrm{GdFe}}\left(\frac{\partial\theta(z)}{\partial z}\right)^2+K_{\mathrm{GdFe}}\sin^2\theta(z)-HM_{\mathrm{GdFe}}\cos\theta(z)\right]dz+\int_{t_{\mathrm{GdFe}}}^{t_{\mathrm{GdFe}}+t_{\mathrm{TbFe}}}\left[A_{\mathrm{TbFe}}\left(\frac{\partial\theta(z)}{\partial z}\right)^2+K_{\mathrm{TbFe}}\sin^2\theta(z)-HM_{\mathrm{TbFe}}\cos\theta(z)\right]dz+J\cos(\theta^i_{\mathrm{TbFe}}-\theta^i_{\mathrm{GdFe}}),$$

where θ^i_{GdFe} and θ^i_{TbFe} are, respectively, the angle of the magnetization at the interface in GdFe and in the TbFe layer. We determined the magnetic profiles which minimize the energy (stable and metastables states) from which we calculated the magnetization M and the susceptibility $\partial M/\partial H$. The magnetic parameters used for the calculation are summarized in Table I.

Magnetic measurements were first performed at 300 K to establish the possible initial magnetic configurations before cooling the sample under a magnetic field H_{fc}. Experimental results are reported in Fig. 1 for both magnetization and susceptibility. The hysteresis loops as a function of the applied magnetic field are plotted along with the results of the micromagnetic calculations. For the clarity of the figure, only the absolute minimum-energy solution is represented. The agreement between measurement and micromagnetic calculations is then very good for both magnetization and susceptibility. The solutions corresponding to local minima (not represented in Fig. 1) reproduce satisfactorily the opening of the loops. The magnetic profile $\theta(z)$ from the calculation for five different fields are presented in inset in Fig. 2. For very large positive fields ($H=70$ kOe), both magnetizations point in the field direction with only a small shift at the interface, consequently the angle between the interface GdFe and TbFe magnetizations and the field direction are close to zero ($\theta^i_{\mathrm{GdFe}}\simeq0°$ and $\theta^i_{\mathrm{TbFe}}\simeq0°$). As the field is decreased the balance between Zeeman energy and the interfacial antiferromagnetic coupling leads to the formation of an iDW, mainly located in the TbFe layer (inset of Fig. 2). Its thickness increases and θ^i_{TbFe} (calculated) rises from 0° angle toward 180° (Fig. 2). This ''decompression'' of the iDW is slightly visible from the slow decrease of the magnetization, but it is clearly evidenced by the susceptibility measurements. Indeed, when a DW becomes larger, the amount of magnetization having a component perpendicular to the field direction increases, which increases the susceptibility.[12] The susceptibility is maximum at $H=100$ Oe field at which the antiferromagnetic coupling takes over the Zeeman energy and the TbFe magnetization reverses abruptly (Fig. 1). The magnetizations are thus antiparallel and entirely along the applied field ($\theta^i_{\mathrm{GdFe}}=0°$ and $\theta^i_{\mathrm{TbFe}}=180°$) without any iDW. This transition leads to a drop of the susceptibility because of the disappearance of transverse magnetization component. For a small negative field, the whole structure (GdFe and TbFe still antiferromagntically aligned) reverses its magnetization (Fig. 2), GdFe magnetization is now pointing in the negative field direction ($\theta^i_{\mathrm{GdFe}}=180°$ and $\theta^i_{\mathrm{TbFe}}=0°$). For $H<-200$ Oe, Zeeman energy takes over interfacial cou-

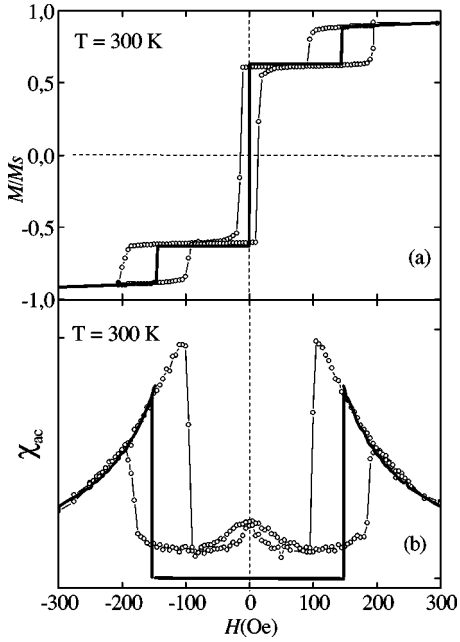

FIG. 1. Normalized magnetization M/M_S (a) and susceptibility χ_{ac} (b) as a function of the magnetic field H applied along the easy axis for $Gd_{40}Fe_{60}$(100 nm)/$Tb_{12}Fe_{88}$(50 nm) at 300 K. Experimental data (open circle) are compared to calculated values (solid line).

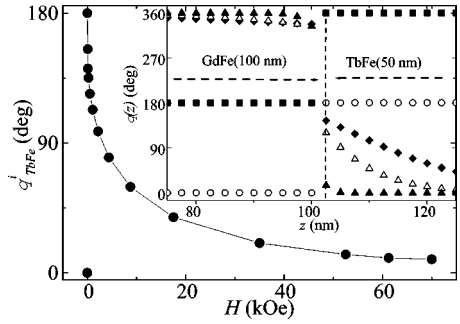

FIG. 2. Calculated angle θ^i_{TbFe} between the TbFe interface spin and the cooling field direction as a function of the applied field H. In inset, magnetic configurations in the GdFe/TbFe bilayer at 300 K, $\theta(z)$, for various fields 70 kOe (full triangle), 1 kOe (open triangle), 150 Oe (full diamond), and 0 Oe. For the zero field two configurations are possible (open circle) and (full square).

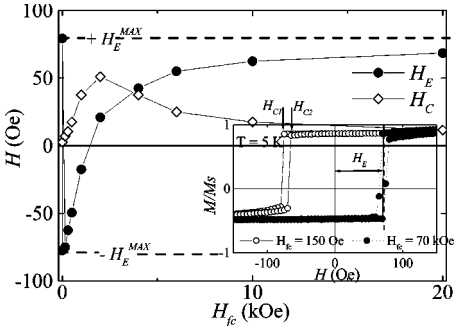

FIG. 3. Variation of the exchange bias field H_E and the coercive field H_C as a function of the cooling field H_{fc}. In inset, hysteresis loops at 5 K for $H_{fc}=70$ kOe and $H_{fc}=150$ Oe. H_{C1} and H_{C2} are defined for $H_{fc}=150$ Oe

pling and the TbFe magnetization aligns along the field, leading again to the creation of an iDW. Symmetric behavior is observed while the field is swept back to positive. The room-temperature behavior of the GdFe/TbFe bilayer is similar to the one obtained for GdFe/FeSn antiferromagnetically coupled systems.[15] It is thus perfectly understood and conform to a simple micromagnetic model which allows to predict the magnetic configuration at the TbFe interface, and particularly θ^i_{TbFe} represented in Fig. 2.

The sample was then cooled down to 5 K under constant magnetic fields H_{fc}. Two examples of 5 K hysteresis loop are represented in the inset of Fig. 3. The net bias field appearing in the cycle depends clearly on the cooling field H_{fc}. This phenomenon is accompanied by a magnetization shift, whose variation with H_{fc} is reported in Fig. 4(b). The two switching fields H_{C1} and H_{C2} are plotted as a function of H_{fc} in Fig. 4(a). As usual, we define $H_E=(H_{C2}+H_{C1})/2$ and the coercivity as $H_C=(H_{C2}-H_{C1})/2$, both plotted in Fig. 3 as a function of the cooling field. The exchange field is maximal in negative values ($H_E=-H_E^{max}$) for $H_{fc}=0$ ($\theta^i_{\mathrm{TbFe}}=180°$) and increases monotonically with H_{fc}. It is remarkable that for large values of H_{fc} ($\theta^i_{\mathrm{TbFe}}=0°$), H_E tends toward $+H_E^{max}$ (which is also the exchange field for $H_{fc}=0$ with $\theta^i_{\mathrm{TbFe}}=0°$). H_C is minimum for low and large values of H_{fc} and maximum for an intermediate value corresponding to an H_{fc} for which H_E is almost zero. It appears clearly that H_E is related to H_{fc} and particularly to the interface magnetic configuration in the TbFe before the cooling. Indeed from $H_E=-H_E^{max}$ for $\theta^i_{\mathrm{TbFe}}=180°$, H_E increases to $+H_E^{max}$ for $\theta^i_{\mathrm{TbFe}}=0°$ going through $H_E=0$ for about $\theta^i_{\mathrm{TbFe}}=\pm 90°$.

To quantify this relationship, we suppose below that the 300-K magnetic configuration inside the TbFe is frozen during the cooling procedure and remained unchanged at 5 K. Consequently, $\theta^i_{\mathrm{TbFe}}(H=H_{fc})$ at 300 K is equal to $\theta^i_{\mathrm{TbFe}}(H_{fc})$ at 5 K. Micromagnetic calculations have been performed for various fixed TbFe configurations deduced from 300 K calculations and using GdFe magnetic parameters for 5 K (Table I) considering that the magnetization of TbFe is frozen. The field H_{C1}^{calc} for which it is energetically favorable for the GdFe magnetization to reverse was then deduced and found to be a linear function of θ^i_{TbFe}. The

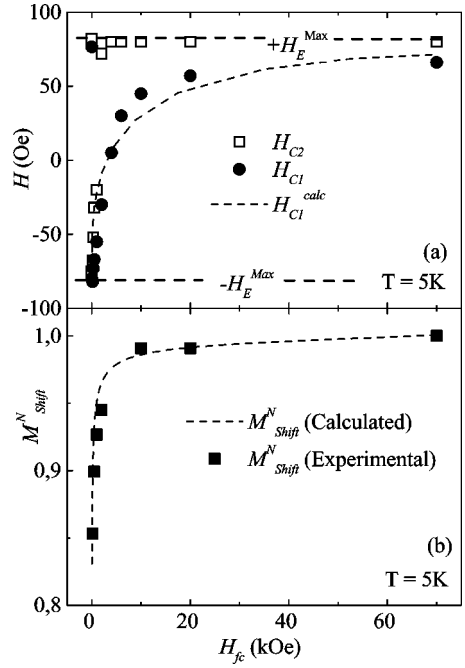

FIG. 4. (a) Evolution of the calculated field H_{C1}^{calc} at which GdFe reverses (dash line) compared to H_{C1} (full circle) and H_{C2} (open square) as a function of the cooling field H_{fc}. (b) Cooling field dependence of the experimental (full square) and calculated (dash line) normalized magnetization shift $M^N_{Shift}(H_{fc})$.

H_{C1}^{calc} variation as a function of H_{fc} is compared to H_{C1} variation in Fig. 4(a). The agreement between the experimental results and the frozen magnetic configuration hypothesis is good, showing the relevance of iDW to explain exchange bias phenomena in our system. The difference between H_{C2} and H_{C1}, the coercivity, is superior to the intrinsic coercivity of GdFe and upon a certain value of cooling field ($H_{fc}>4$ kOe), H_{C2} is constant and equal to $+H_E^{max}$. These points suggest that during the GdFe reversal at H_{C1}, a rearrangement of the TbFe interface magnetization occurs with a reduction of θ^i_{TbFe}. For $\theta^i_{\mathrm{TbFe}}<90°$ (corresponding to $H_{fc}>4$ kOe), the rearrangement leads directly to $\theta^i_{\mathrm{TbFe}}=0°$ and $H_{C2}=+H_E^{max}$. The amplitude of the rearrangement is directly given by the coercivity (represented in Fig. 3). The amplitude is maximum for low exchange bias fields. The torque "exerted" by the GdFe during its reversal on the TbFe interface is thus maximum for $\theta^i_{\mathrm{TbFe}}=90°$. Nevertheless, this rearrangement does not limit our quantitative analysis in first stage of the M-H loop.

Let us point out that the results described above for $Gd_{40}Fe_{60}/Tb_{12}Fe_{88}$ are in all respect similar to previous observations done on Fe/FeF_2 and $Fe/FeMn_2$ systems.[4,5] It actually gives credit to new theoretical and experimental development[18] showing that in the AFM the moments tend to align along the field axis as it is the case for TbFe. Moreover, the magnetization shift [Fig. 4(b)] observed in both systems can be easily explained by our model. Indeed the presence of the interfacial DW changes the net magnetization of the system. We then defined the normalized magnetization shift $M^N_{Shift}(H_{fc})$ for a given cooling field H_{fc} as $M^N_{Shift}(H_{fc})$

$=M_{2\ \mathrm{kOe}}(H_{fc})/M_{2\ \mathrm{kOe}}(H_{fc}=70\ \mathrm{kOe})$ where $M_{2\ \mathrm{kOe}}(H_{fc})$ is the magnetization measured at 5 K under 2 kOe after cooling the sample from 300 K under H_{fc}. The calculated and experimental results are in very good agreement as shown in Fig. 4. Moreover for Fe/FeF_2 and $Fe/FeMn_2$, the H_{fc} dependence of the magnetization shift is qualitatively the same. However, because the net magnetization of AFM is zero, this shift is about 1% of the total magnetization whereas in our case it reaches 10%.

In conclusion, by using a ferrimagnetic/ferrimagnetic bilayer, we have investigated the magnetic configurations inside an exchange-coupled bilayer system at a temperature (T=300 K) above the blocking temperature for which exchange bias appears. The cooling field dependence of the exchange bias phenomena (H_E, H_C, M^N_{Shift}) were then explained considering laterally uniform magnetization and the freezing of the magnetic configuration in the pinning layer (TbFe). However no lateral domain formation in either of the two layer is required. More precisely the exchange bias field value is dominated by the angle between the magnetization of the interface pinned layer and the cooling field direction, whereas the magnetization shift is related to the interface magnetic configuration. The model developed here for antiferromagnetically coupled bilayers may be transposed from ferrimagnetic/ferrimagnetic to FM/AFM systems which explains all the reported experimental results for Fe/FeF_2 and Fe/MnF_2 systems and gives credit to interface domain-wall models.[9–11]

We thank M. Hehn and Y. Henry for interesting and fruitful discussions, L. Joly for his help in the micromagnetic calculations, and M. Alnot, F. Mouginet, and D. Pierre for help with experiments.

[1] W.H. Meiklejohn and C.P. Bean, Phys. Rev. **105**, 904 (1957).
[2] A.E. Berkowitz and K. Takano, J. Magn. Magn. Mater. **200**, 552 (1999); J. Nogues and I.K. Schuller, *ibid.* **192**, 203 (1999); M. Kiwi, *ibid.* **234**, 584 (2001).
[3] J.R. Childress *et al.*, IEEE Trans. Magn. **37**, 1745 (2001).
[4] J. Nogues, D. Lederman, T.J. Moran, and Ivan K. Schuller, Phys. Rev. Lett. **76**, 4624 (1996).
[5] J. Nogues, C. Leighton, and I.K. Schuller, Phys. Rev. B **61**, 1315 (2000).
[6] C. Leighton, M.R. Fitzsimmons, A. Hoffmann, J. Dura, C.F. Majkrzak, M.S. Lund, and I.K. Schuller, Phys. Rev. B **65**, 064403 (2002); C. Leighton, J. Nogues, B.J. Josson-Akerman, and I.K. Schuller, Phys. Rev. Lett. **84**, 3466 (2000).
[7] T.L. Kirk, O. Hellwig, and E.E. Fullerton, Phys. Rev. B **65**, 224426 (2002).
[8] A.P. Malozemoff, J. Appl. Phys. **63**, 3874 (1988).
[9] D. Mauri, H.C. Siegmann, P.S. Bagus, and E. Kay, J. Appl. Phys. **62**, 3047 (1987).
[10] M. Kiwi, J. Mejia-Lopez, R.D. Portugal, and R. Ramirez, Europhys. Lett. **48**, 573 (1999).
[11] R.L. Stamps, J. Magn. Magn. Mater. **242-245**, 139 (2002).
[12] S. Mangin, G. Marchal, and B. Barbara, Phys. Rev. Lett. **82**, 4336 (1999).
[13] E.E. Fullerton, J.S. Jiang, M. Grimsditch, C.H. Sowers, and S.D. Bader, Phys. Rev. B **58**, 12 193 (1998).
[14] F. Montaigne, S. Mangin, and Y. Henry, Phys. Rev. B **67**, 144412 (2003).
[15] F. Canet, S. Mangin, C. Bellouard, and M. Piecuch, Europhys. Lett. **52**, 594 (2000).
[16] P. Hansen, C. Clausen, G. Much, M. Rosenkranz, and K. Witter, J. Appl. Phys. **66**, 756 (1989).
[17] S. Mangin, C. Bellouard, G. Marchal, and B. Barbara, J. Magn. Magn. Mater. **165**, 161 (1997).
[18] U. Nowak, K.D. Usadel, J. Keller, P. Miltnyi, B. Beschoten, and G. Guntherodt, Phys. Rev. B **67**, 014430 (2002).